

AD\_\_\_\_\_

Award Number: DAMD17-00-1-0245

TITLE: Robust Detection of Masses in Digitized Mammograms

PRINCIPAL INVESTIGATOR: Lihua Li

CONTRACTING ORGANIZATION: University of South Florida  
Tampa, Florida 33620

REPORT DATE: June 2004

TYPE OF REPORT: Annual Summary

PREPARED FOR: U.S. Army Medical Research and Materiel Command  
Fort Detrick, Maryland 21702-5012

DISTRIBUTION STATEMENT: Approved for Public Release;  
Distribution Unlimited

The views, opinions and/or findings contained in this report are those of the author(s) and should not be construed as an official Department of the Army position, policy or decision unless so designated by other documentation.

**20050819069**

**REPORT DOCUMENTATION PAGE**Form Approved  
OMB No. 074-0188

Public reporting burden for this collection of information is estimated to average 1 hour per response, including the time for reviewing instructions, searching existing data sources, gathering and maintaining the data needed, and completing and reviewing this collection of information. Send comments regarding this burden estimate or any other aspect of this collection of information, including suggestions for reducing this burden to Washington Headquarters Services, Directorate for Information Operations and Reports, 1215 Jefferson Davis Highway, Suite 1204, Arlington, VA 22202-4302, and to the Office of Management and Budget, Paperwork Reduction Project (0704-0188), Washington, DC 20503

<b>1. AGENCY USE ONLY</b> (Leave blank)		<b>2. REPORT DATE</b> June 2004	<b>3. REPORT TYPE AND DATES COVERED</b> Annual Summary (15 May 2000 - 14 May 2004)	
<b>4. TITLE AND SUBTITLE</b> Robust Detection of Masses in Digitized Mammograms			<b>5. FUNDING NUMBERS</b> DAMD17-00-1-0245	
<b>6. AUTHOR(S)</b> Lihua Li, Ph.D.				
<b>7. PERFORMING ORGANIZATION NAME(S) AND ADDRESS(ES)</b> University of South Florida Tampa, Florida 33620  <b>E-Mail:</b> lilh@moffitt.usf.edu			<b>8. PERFORMING ORGANIZATION REPORT NUMBER</b>	
<b>9. SPONSORING / MONITORING AGENCY NAME(S) AND ADDRESS(ES)</b> U.S. Army Medical Research and Materiel Command Fort Detrick, Maryland 21702-5012			<b>10. SPONSORING / MONITORING AGENCY REPORT NUMBER</b>	
<b>11. SUPPLEMENTARY NOTES</b>				
<b>12a. DISTRIBUTION / AVAILABILITY STATEMENT</b> Approved for Public Release; Distribution Unlimited				<b>12b. DISTRIBUTION CODE</b>
<b>13. ABSTRACT (Maximum 200 Words)</b> This project is to develop a robust computer aided diagnosis (CAD) system for mass detection with high sensitivity and specificity in digitized mammograms. The research in fourth year is on data collection, evaluation of clinical significance of CAD system, and the final documentation and manuscript reports. By reviewing more than 1334 cases, a total of 83 serial cancer cases were collected. A group truth file was generated by an experienced radiologist. This work is continuing and more cases will be collected to achieve the goal of 100 cases before the end of May 2004. However, due to the difficulty and the huge working load in database generation, the testing of clinical significance of CAD system could not be finished in this year. We are requesting a no-cost extension of this grant. The results of this part will be reported in the final report next year.				
<b>14. SUBJECT TERMS</b> Breast cancer, mass, detection, CAD, Mammography, robust, adaptive, segmentation, classification				<b>15. NUMBER OF PAGES</b> 16
				<b>16. PRICE CODE</b>
<b>17. SECURITY CLASSIFICATION OF REPORT</b> Unclassified	<b>18. SECURITY CLASSIFICATION OF THIS PAGE</b> Unclassified	<b>19. SECURITY CLASSIFICATION OF ABSTRACT</b> Unclassified	<b>20. LIMITATION OF ABSTRACT</b> Unlimited	

## Table of Contents

Cover.....	1
SF 298.....	2
Table of Contents.....	3
Introduction.....	4
Body.....	4
Key Research Accomplishments.....	7
Reportable Outcomes.....	7
Conclusions.....	8
References.....	
Appendices.....	9

## INTRODUCTION

This project is to develop a robust computer aided diagnosis (CAD) system for mass detection with high sensitivity and specificity in digitized mammograms. As listed in the Statement of Work, the research scope in the fourth year of project is to evaluate the clinical significance of CAD system and finish the final documentation and manuscript reports. This study is to be taken by testing how well the CAD algorithm performs in early detection of masses with a consecutive set of mammograms.

## BODY

***Objective 1: to generate a database containing 100 consecutive cases for evaluation of clinical significance of CAD system.***

### **Accomplishments:**

#### **1. Data Collection Criteria and Procedure**

In order to test the clinical significance of CAD system in terms of early detection, a serial data set of mammograms was collected, in which each case contains a minimum of 2 consecutive mammograms with masses. The criteria for inclusion in this study were as follows:

1. Mass must be visible on mammogram
2. Mass must be proven by biopsy to be malignant
3. Mass must be seen in retrospect on a prior mammogram when reviewed by a radiologist

Procedure used for case selection consists of

1. Lists of patients from both the screening and diagnostic centers were obtained
2. Each patient's chart was reviewed to select for masses that were visible mammographically, all others were excluded
3. The selected cases were reviewed for malignant pathology outcome, all others were excluded
4. Films were requested from the diagnostic center for those cases with malignant masses
5. Films from the screening center had to be obtained manually due to lack of manpower
6. Films were reviewed to ascertain whether the exam and prior mammograms were available. Only those with prior mammograms were selected.
7. Selected mammograms were reviewed by a radiologist to determine a) if the mass was visible retrospectively on the prior exam and b) the reason it was not detected on the prior exam
8. The radiologist indicated the location and outlined the contour of the lesion on both exams and the BIRADS descriptors
9. Ground truth files (hard copy) were generated based on the radiologists outlines
10. The films were then digitized manually on a Kodak (LUMISYS) LS85 digitizer at a resolution of 50 $\mu$ m and 12 bits in grey scale.

#### **2. Sources and number of cases reviewed: (as of March 23, 2004)**

Query of patient databases	770
Staging database	93
Teaching files archive	148
Breast conference patients	100
Log of invasive procedures	160

Research archives	63
<b>Total number of cases reviewed</b>	<b>1,334</b>

### 3. Reasons for exclusion of cases from the original 1,334 patients reviewed:

Duplication of names among lists  
 Lesion was something other than a mass  
 Lesion was a benign mass  
 No pathology available  
 No information available for this patient/exam  
 No follow up for this patient  
 Films were unavailable or incomplete  
 Mass was not visible on prior mammogram (interval cancer)

#### *a. Analysis of the 770 names from patient database queries:*

<b>Reason</b>	<b>Number excluded</b>
Duplication of names among lists	49
Lesion was something other than a mass	337
Lesion was a benign mass	111
No information available	51
No follow up available	56

-----  
 This leaves a balance of 166 potential cases, of which:

Films were unavailable or incomplete	100
Mass not visible on prior exam	16
Miscellaneous exclusions	21

<b>Usable cases</b>	<b>29</b>
---------------------	-----------

#### *b. Analysis of the 93 names from the staging database:*

<b>Reason</b>	<b>Number excluded</b>
Duplication of names among lists	1
Lesion was something other than a mass	39
No information available	9

-----  
 This leaves a balance of 44 potential cases, of which:

Films were unavailable or incomplete	42
--------------------------------------	----

<b>Usable cases</b>	<b>2</b>
---------------------	----------

#### *c. Analysis of the 148 names from teaching files:*

<b>Reason</b>	<b>Number excluded</b>
Duplication of names among lists	20
Lesion was something other than a mass	58
Lesion was a benign mass	12
No information available	13
No pathology available	1

-----  
 This leaves a balance of 44 potential cases, of which:

Films were unavailable or incomplete	32
Mass not visible on prior exam	5

**Usable cases****7*****d. Analysis of the 100 names from breast conference lists:***

<b>Reason</b>	<b>Number excluded</b>
Duplication of names among lists	8
Lesion was something other than a mass	34
Lesion was a benign mass	1
No information available	12

---

This leaves a balance of 45 potential cases, of which:

Films were unavailable or incomplete	29
Mass not visible on prior exam	4

**Usable cases****12*****e. Analysis of the 160 names from invasive procedures log:***

<b>Reason</b>	<b>Number excluded</b>
Duplication of names among lists	4
Lesion was something other than a mass	71
Lesion was a benign mass	4
No information available	20

---

This leaves a balance of 61 potential cases, of which:

Films were unavailable or incomplete	34
Mass not visible on prior exam	5

**Usable cases****22*****f. Analysis of the 63 names from research archives:***

<b>Reason</b>	<b>Number excluded</b>
Duplication of names among lists	2
Lesion was something other than a mass	22
Lesion was a benign mass	5
No pathology available	9

---

This leaves a balance of 25 potential cases, of which:

Mass not visible on prior exam	11
--------------------------------	----

**Usable cases****14**

**Summary:** As of the end of March 2004, a total of 86 out of 1334 cases were collected as consecutive cancer cases for study. Since then, there are another 6 cases have been collected, but the electronic truth files need to be generated. It is anticipated that we can achieve the goal of 100 cases by the end of May 2004.

**4. Characteristic analysis of the database**

The characteristics of database was analyzed by following descriptions: (a) Case distribution in terms of exam numbers, (b) Case distribution in terms of mass shape, (c) Case distribution in terms of mass margin, (d) Case distribution in terms of Mass density. The histograms are shown in Figure 1.

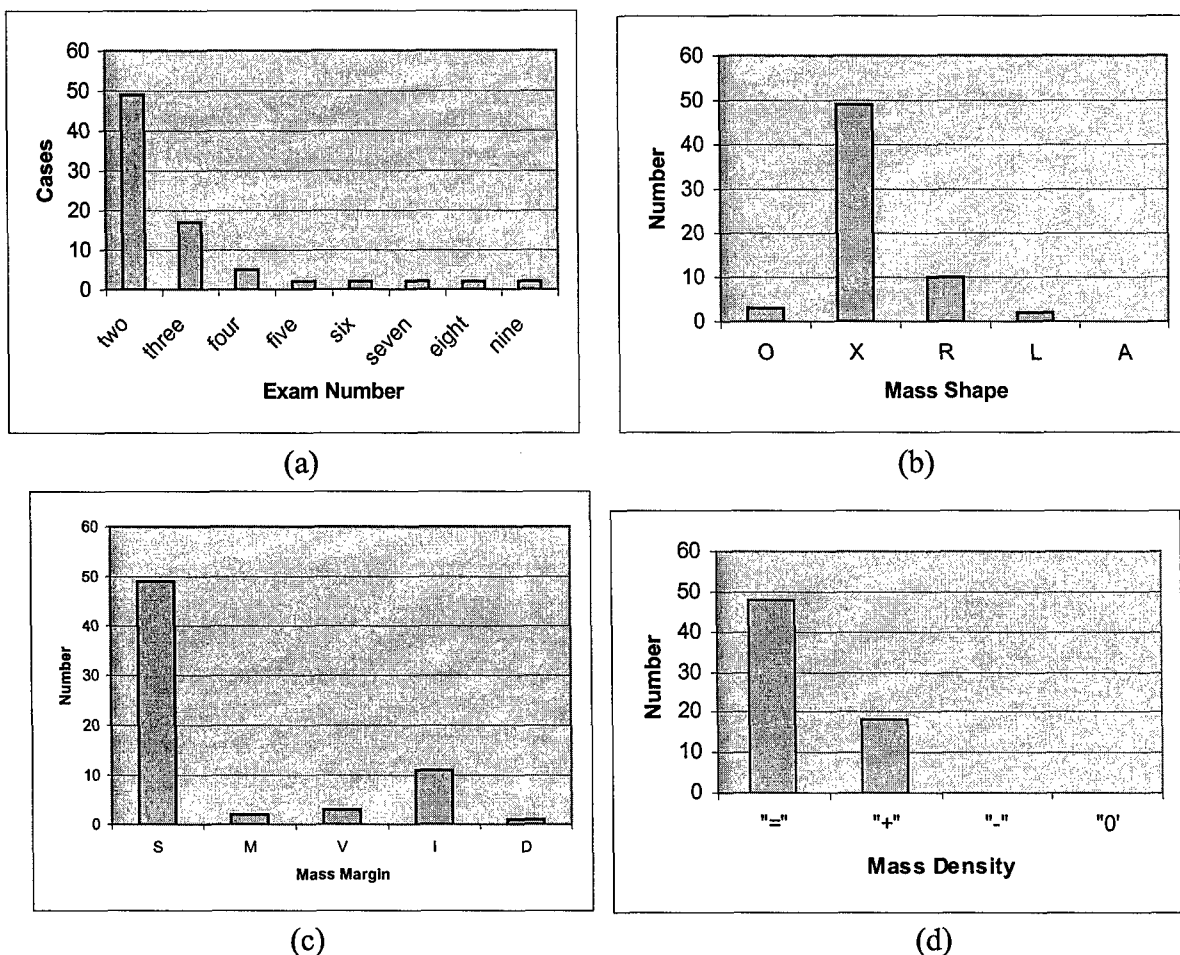


**Figure 1.** Case distribution in terms of (a) exam numbers, (b) mass shape, (c) mass margin, (d) Mass density.

***Objective 2: evaluation of clinical significance of CAD system in terms of early detection***

Due to the unexpected difficulty and the huge working load in serial data collection, the evaluation of clinical significance of CAD system could not be finished at this time. We are requesting a no-cost extension of this grant. The results of this part will be reported in the final report next year.

**KEY RESEARCH ACCOMPLISHMENTS**

1. A database of mammogram was generated containing 83 cases of serial mammograms, which were selected by reviewing more than 1334 cases.
2. An analysis of collected database was taken in terms of consecutive exam number, mass shape, mass margin, and mass density.

**REPORTABLE OUTCOMES**

*1. Presentation and/or proceedings paper*

(a) Y. Qiu, L. Li, D. Goldgof, R.A. Clark, "Three dimensional deformation model for lesion correspondence in breast imaging," Proceedings of SPIE Medical Imaging, 2003.

## *2. Fundings Applied*

(a) "Computer Aided Diagnosis of Focal Asymmetric Density", a project in Program Grant titled "Breast Imaging and Computerized Analysis Program" submitted to NCI, 2003.

## **CONCLUSIONS**

This project is to develop a robust computer aided diagnosis (CAD) system for mass detection with high sensitivity and specificity in digitized mammograms. The research in fourth year is on data collection, evaluation of clinical significance of CAD system, and the final documentation and manuscript reports. By reviewing more than 1334 cases, a total of 83 serial cancer cases were collected. A ground truth file was generated by an experienced radiologist. This work is continuing and more cases will be collected to achieve the goal of 100 cases before the end of May 2004. However, due to the difficulty and the huge working load in database generation, the testing of clinical significance of CAD system could not be finished in this year. We are requesting a no-cost extension of this grant. The results of this part will be reported in the final report next year.

# Three Dimensional Finite Element Model for Lesion Correspondence in Breast Imaging

Yan Qiu, Lihua Li, Dmitry Goldgof\*, Sudeep Sarkar\*, Sorin Anton\*, Robert A. Clark

Department of Radiology, College of Medicine,  
H. Lee Moffitt Cancer Center & Research Institute  
University of South Florida, Tampa, FL 33612

\* Department of Computer Science and Engineering  
University of South Florida, Tampa, FL 33620, USA

## ABSTRACT

Predicting breast tissue deformation is of great significance in several medical applications such as biopsy, diagnosis, and surgery. In breast surgery, surgeons are often concerned with a specific portion of the breast, e.g., tumor, which must be located accurately beforehand. Also clinically it is important for combining the information provided by images from several modalities or at different times, for the detection/diagnosis, treatment planning and guidance of interventions. Multi-modality imaging of the breast obtained by X-ray mammography, MRI is thought to be best achieved through some form of data fusion technique. However, images taken by these various techniques are often obtained under entirely different tissue configurations, compression, orientation or body position. In these cases some form of spatial transformation of image data from one geometry to another is required such that the tissues are represented in an equivalent configuration.

We propose to use a 3D finite element model for lesion correspondence in breast imaging. The novelty of the approach lies in the following facts: (1) Finite element is the most accurate technique for modeling deformable objects such as breast. The physical soundness and mathematical rigor of finite element method ensure the accuracy and reliability of breast modeling that is essential for lesion correspondence. (2) When both MR and mammographic images are available, a subject-specific 3D breast model will be built from MRIs. If only mammography is available, a generic breast model will be used for two-view mammography reading. (3) Incremental contact simulation of breast compression allows accurate capture of breast deformation and ensures the quality of lesion correspondence. (4) Balance between efficiency and accuracy is achieved through adaptive meshing. We have done intensive research based on phantom and patient data.

**Keywords:** Finite Element Method, Mammogram, MRI, Lesion correspondence

## 1. INTRODUCTION

Breast cancer is the second leading cause of cancer death for all women (after lung cancer), and the leading overall cause of cancer death in women between the ages of 40 and 59. In 2002, 257,800 new cases of breast cancer will be diagnosed, and 39,600 women will die from the disease. The risk of developing breast cancer seems to depend on several factors including age, personal or family history of breast cancer, parity, age at first birth, hormonal replacement, etc. However, over 70% of cancer cases are women with no identifiable risk factors. Early diagnosis is very important for proper treatment and cure and this has led many countries, including US, to develop regular screening programs that are primarily based on mammography and physical examination [1, 2].

Mammography is the main screening tool for breast cancer with a sensitivity of about 85% and specificity up to 25%. Despite their proven effectiveness, both screening tools entail significant variability and there are few attempts to-date to standardize either one or correlate mammographic to physical examination findings. Techniques that improve the accuracy of mammography or physical breast examination or both are still highly desirable and could benefit breast cancer diagnose. Furthermore, methodologies that yield a 3D representation of the breast with accurate volume and lesion location are

expected to offer a unique tool for accurate and consistent follow-up, for correlation between findings from different screening procedures, as well as correlation of serial examinations (annual or serial exams).

Screening mammograms usually consist of a craniocaudal (CC) and mediolateral oblique (ML) view of each breast. Breast x-rays show areas of fatty and glandular tissue, pectoral muscle (if the view is ML), skin boundary, nipple and the non-breast region. Due to variation in compression and physical changes of the breast, consecutive mammograms of the same patient are difficult to fully correlate from one examination to the next and the expert reader may identify only general similarities. Similarly, due to differences in compression geometry and lack of common, reference points or fixed landmarks other than the nipple, one-to-one correspondence between the mammographic views is nearly impossible, and well-known stereo imaging algorithms widely used in stereo navigation, such as stereovision or passive ranging, cannot be applied to mammography.

We propose to construct solid model for human breast, and design solid model-based methods to estimate non-rigid registration and non-rigid motion attributes, that is, to predict physical deformation and displacements of the breast and perform a non-rigid registration between two different X-ray views. This is useful for surgical procedures and diagnoses purposes. A 3D finite element model of the breast was constructed based on the MR slice images. With FEM model, a compression similar to one performed during mammography data acquisition, was simulated and a registration between the projected image of 3D volume and X-ray images was performed.

Two types of model have been used in two-view mammography: statistical and geometrical. In statistical model-based approach, a classifier can be trained through similarity analysis among feature pairs identified in two views and then be used to help single-view detection. This approach has the drawbacks that only limited geometrical information of features can be utilized, which affects its accuracy and reliability. Geometrical model has also been used to facilitate two-view feature registration and 3D reconstruction of calcification [3,4,5]. The disadvantage of geometrical model is that many assumptions must be made to idealize breast deformation. The assumptions may be invalid for breasts that had large non rigid deformation during X-ray imaging. 3D finite element model is proposed to be used for two-view mammography interpretation [6, 7, 8, 9].

## 2. FINITE ELEMENT MODEL

Finite element method is a technique for modeling deformable objects such as breast [10, 11, 12, 13, 14]. The physical soundness and mathematical rigor of finite element method ensure the accuracy and reliability of breast modeling that is essential for two-view mammography reading. When both MR and mammographic images are available, a subject-specific 3D breast model can be built from MRI. If only mammography is available, a generic breast model can be used for two-view mammography reading.

The breast deformation can be described by:

$$(\lambda + G)\nabla(\nabla \cdot \mathbf{u}) + G\nabla^2 \mathbf{u} + \mathbf{F} = \rho \frac{\partial^2 \mathbf{u}}{\partial t^2} \quad (1)$$

where  $\mathbf{u}$  is displacement,  $\mathbf{F}$  is force,  $t$  is time,  $\rho$  is mass, and  $(G, \lambda)$  are Lamè constants. After finite element discretization, we obtain a transient matrix equation:

$$\mathbf{M}\ddot{\mathbf{u}} + \mathbf{C}\dot{\mathbf{u}} + \mathbf{K}\mathbf{u} = \mathbf{F}(t) \quad (2)$$

where  $\mathbf{M}$  is mass matrix,  $\mathbf{C}$  is damping matrix,  $\mathbf{K}$  is stiffness matrix that is composed of material properties, and  $\mathbf{F}(t)$  is force. In static case, it becomes  $\mathbf{K}\mathbf{u} = \mathbf{F}$ , which will be used in breast deformation modeling.

The FEM is discretized using unstructured tetrahedral element because of its computational efficiency and flexibility in handling complex shapes. 10-node tetrahedral element is used to increase modeling accuracy for large breast deformation. The dynamics of the elastic body is governed by the following system of partial differential equations:

$$\begin{aligned} \rho_0 \frac{\partial^2 \mathbf{u}}{\partial t^2} &= (\lambda + \mu) \left( \frac{\partial^2 \mathbf{u}}{\partial x^2} + \frac{\partial^2 \mathbf{v}}{\partial y \partial x} + \frac{\partial^2 \mathbf{w}}{\partial z \partial x} \right) + \mu \nabla^2 \mathbf{u} + \mathbf{f}_x \\ \rho_0 \frac{\partial^2 \mathbf{v}}{\partial t^2} &= (\lambda + \mu) \left( \frac{\partial^2 \mathbf{u}}{\partial x \partial y} + \frac{\partial^2 \mathbf{v}}{\partial y^2} + \frac{\partial^2 \mathbf{w}}{\partial z \partial y} \right) + \mu \nabla^2 \mathbf{v} + \mathbf{f}_y \\ \rho_0 \frac{\partial^2 \mathbf{w}}{\partial t^2} &= (\lambda + \mu) \left( \frac{\partial^2 \mathbf{u}}{\partial x \partial z} + \frac{\partial^2 \mathbf{v}}{\partial y \partial z} + \frac{\partial^2 \mathbf{w}}{\partial z^2} \right) + \mu \nabla^2 \mathbf{w} + \mathbf{f}_z \end{aligned} \quad (3)$$

where:  $(u,v,w)$  – 3D displacement vector,  $f_i$  - force field, and  $\mu, \lambda$  are Lamé constants, computed from Young's modulus and Poisson's ratio.

### 3. ALGORITHM

The objectives of our project are to develop new procedures using 3D deformation model to fulfill following tasks:

- Increase the accuracy in the registration and correlation of the mammographic views.
- Provide accurate localization of findings from mammography or physical examination procedures that could be used for biopsy procedures or follow-up.
- Register MR data sets of the phantom imaged with different amounts of compression.

The main idea of the proposed algorithm is to utilize FEM model of breast constructed from breast MR images to model breast compression during mammographic imaging. Consider a feature point identified in one X-ray view. The location of that point is projected into 3D space and into compressed 3D breast model. The model is uncompressed and the projected line is deformed into a curve. Consider now a feature point in the second X-ray view. Similar projection and decompression of the model is performed and another curve is constructed. If the above two points are views of the same 3D feature point, then those two curves will intersect and that intersection will reconstruct 3D feature point position. If they do not intersect, two points found in each view do not correspond to the same 3D feature point. Fig. 1. illustrates this algorithm. Below we describe two versions of this algorithm.

#### Lesion is visible in 2 views: correspondence recovery

- One feature identified in one view (CC) and its location projected into compressed model as a line
- Model is uncompressed and 3D curve S is constructed
- N features are identified in second view (ML) and all locations are projected into a differently compressed model as line
- Model is uncompressed and N curves are constructed
- Distances between above N curves and curve S are computed
- Minimum distance identifies corresponding features
- Intersection of corresponding 3D curves provides for reconstructed 3D position of this feature.
- All above steps are repeated for all features identified in the first view (CC), all correspondences are identified and all 3D positions are reconstructed.

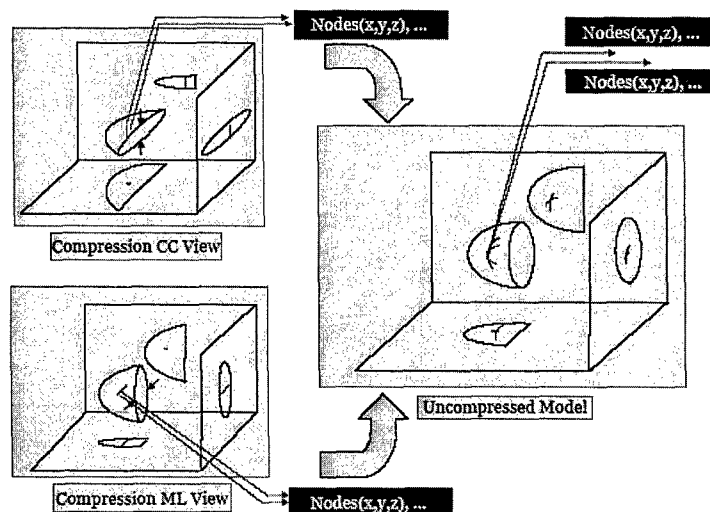


Fig. 1. Correspondence recovery

### Lesion is visible in one view: second reading scenario

- One feature identified in one view (CC) and its location projected into compressed model as a line
- Model is uncompressed and 3D curve is constructed
- Model is compressed for a different view (say ML) and 3D curve is further deformed
- 3D curve is projected into second view (ML), 2D curve is constructed
- The position of the 2D curve indicates where corresponding 2D feature can be located, that area can be marked for the radiologist for second reading. The thickness of the 2D curve is determined by the resolution of the 3D model and the size of feature in the first view (CC). Fig. 2. illustrates this algorithm.

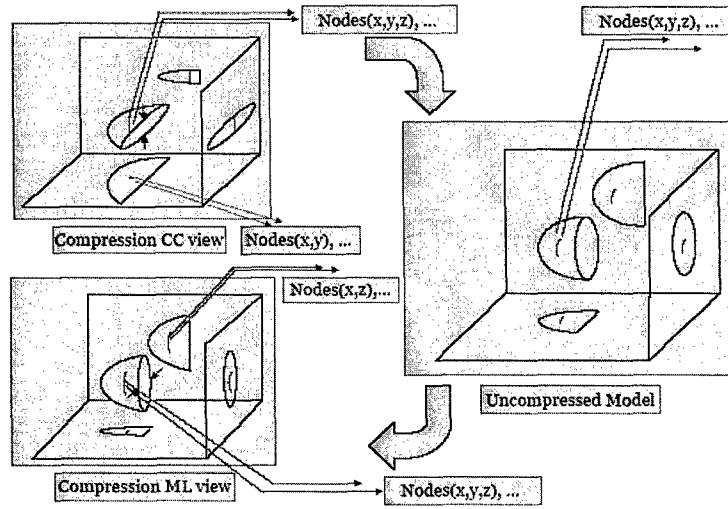


Fig. 2. Second reading

## 4. MODEL CONSTRUCTION

### 4.1 Image Acquisition and Data Extraction

MR volume of phantom is used for model construction and corresponding mammograms are selected for compression simulation experiments. The distance between MR slices is 2.5mm and the voxel size for the T1 MRI is 1.41x1.41x2.50mm. For phantom data experiments we use Triple Modality Biopsy Phantom containing simulated cystic masses and dense masses. Phantom and breast mammograms are scanned at a resolution of 75 micron and 12 bits per pixel.

For each MRI slice, the breast is segmented from background and a 2D breast contour is extracted using standard morphological operators. B-spline smoothing is used to remove small sharp edges that might be generated during segmentation [15,16,17]. The 3D breast shape model is constructed by combining all the 2D breast contours.

### 4.2 Meshing

Voxel- and surface-oriented meshing methods have been used to generate the meshed FEM model. The phantom volume was then meshed into isoparametric tetrahedral structural solids (elements). The elements consist of four corner nodes and an additional node in the middle of each edge. Each node has three associated degrees of freedom (DOF) which define translation into the nodal x-, y- and z-directions. Each element has a quadratic displacement behavior, and provides nonlinear material properties as well as consistent tangent stiffness for large strain applications. The skin was modeled by adding shell elements consisting of eight nodes onto the surface of the fatty tissue. Fig. shows renderings of the FEM models.

The mesh is composed of tetrahedral elements with 10 nodes (each side has an additional node in the middle to model the deformations more accurately) using ANSYS [15, 17, 18, 23, 24, 25, 26]. The elements have a quadratic displacement behavior. The resulting meshed volume is presented in Figure 4. This is the finite element of the phantom to which the deformations will be applied. For a 10 pixels sample interval in the original image slice, 52 slices were stacked to construct the volume and an element size of 8 units. The meshing procedure resulted in 13225 nodes and 8744 elements (see Table. 2.).

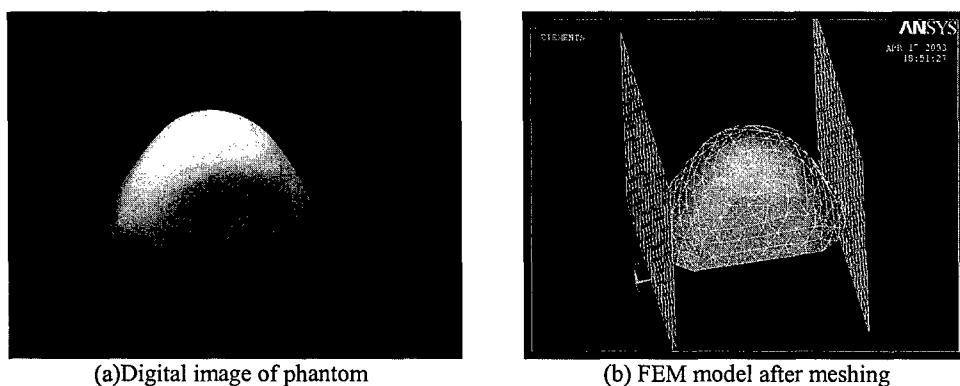


Fig. 3. Finite Element Model for The Phantom

Table 1. Number of Nodes and Elements

Element size	Number of nodes	Number of elements
20	2836	1668
15	4010	2424
10	7899	5068
8	13225	8744
5	52982	36824

#### 4.3 Material Models

To ensure accuracy of breast deformation modeling, appropriate assumptions about material properties of breast tissue must be made. Considering the large deformation caused by compression in X-ray imaging, exponential and polynomial functions are used to account for nonlinear behavior of breast. These functions have been used in many studies on biomechanical modeling of breast [4, 5, 6, 7, 8, 19, 20, 21, 22].

Young's modulus is one of the elastic constants needed to characterize the elastic behavior of a material. Published values of the Young's modulus of component tissue of the breast vary by up to an order of magnitude, presumably due to the method of measurement or estimation. Model calibration is applied in our study to obtain a more accurate value for Poisson's ratio and a smaller error in final registration.

Model calibration is used to train the parameters of the model such that the computed finite element model will have a minimum error comparing with some ground truth. In our case the training parameters are material properties, the model is the breast solid model and the ground truth is the CC X-ray view. In order to calibrate the model, a compression similar to X-ray CC (Cranio-Caudal) view is applied to the breast model and the predicted node displacements are computed. By computing the final registration error the value for Poisson's ratio is updated recursively. After model calibration, Poisson's ratio is set to 0.490.

#### 4.4 Boundary Conditions and Contact Simulation

During X-ray imaging, force is applied through two plates that move towards each other to compress the breast. This is a dynamic contact problem that must be simulated numerically. We approximate breast deformation during compression by incremental stepwise simulation. The underlying assumption is that the motion of plate is slow enough so that breast deformation in each step can be described by a static equilibrium equation. More importantly, the mesh topology will not

be too distorted to affect the displacement prediction. In clinical practice, the final compression magnitude is recorded, but the force exerted on plates is rarely measured. So, we specify Dirichlet condition (displacement) on plates. To avoid sliding movement between plates and breast, we assume that once in contact with plates, the node will move only in the direction of compression. We also assign zero displacement to the nodes that lie on the ribs (chest wall).

## 5. RESULTS AND CONCLUSIONS

X-ray mammograms and MRIs of the breast phantom were used to evaluate the performance of the Finite Element model and the described algorithm. We computed model prediction error as compared to feature size and distance of image features, as illustrated in Table 2.

In experiments of compression simulation using FEM deformation model when suspicious area is visible in 2 views, the smallest distance between curves for 9 feature points we tested is 0.6mm. Ideally the smallest distance between the curves in the uncompressed model should be zero. Compared with the distance between feature points, 25.9mm to 80mm, this result showed that the Finite Element Model can predict lesion correspondence. Validation was also performed using MRI data. The computed lesion coordinates were compared with coordinates calculated from MRI volume set. Distance between a feature point and its prediction is 2.6mm based on 9 feature points in the phantom.

To validate the algorithm for cases when suspicious area is visible only in one view, a feature points visible in both views were selected. First the predicted position is computed (the deformed projected curve), then the minimum Euclidean distance between the real feature position and its prediction is calculated as an indicator for accuracy. The average error is 2.1mm. The average error for MRI volume with simulated compression agreed to within  $1.4\text{mm} \pm 0.3$ .

Table 2. Algorithm performance on phantom data

Simulated Mass and Calcification	Average Error (mm)	Average Feature Diameter (mm)	Average Feature Distance (mm)
3D curve distance	$0.6 \pm 0.4$	10 ~ 20	25.9 ~ 80.0
Predicted 3D lesion position	$2.6 \pm 0.8$	10 ~ 20	25.9 ~ 80.0
Predicted 2D lesion position	$2.1 \pm 0.4$	10 ~ 20	25.9 ~ 80.0
Predicted lesion position in MRI volume	$1.4 \pm 0.3$	10 ~ 20	25.9 ~ 80.0

In conclusion, our initial experiments have shown that we can construct sufficiently detailed 3D FEM model to establish correspondences of features identified in two mammographic views and MRI volume. The proposed algorithm needs to be further tested and validated on larger data set. Further optimization of element sizes and meshing strategies are needed for improved accuracy.

## 6. Appendix

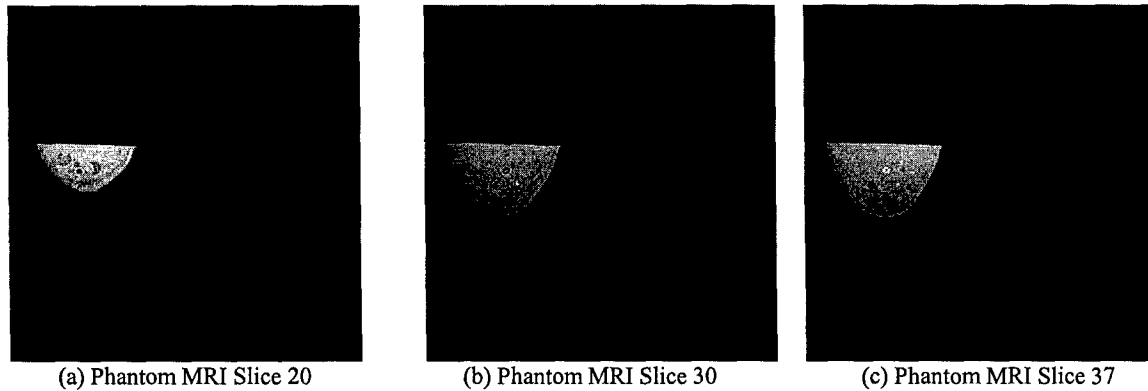


Fig. 4. 52 Phantom MRI Slices for Model Construction

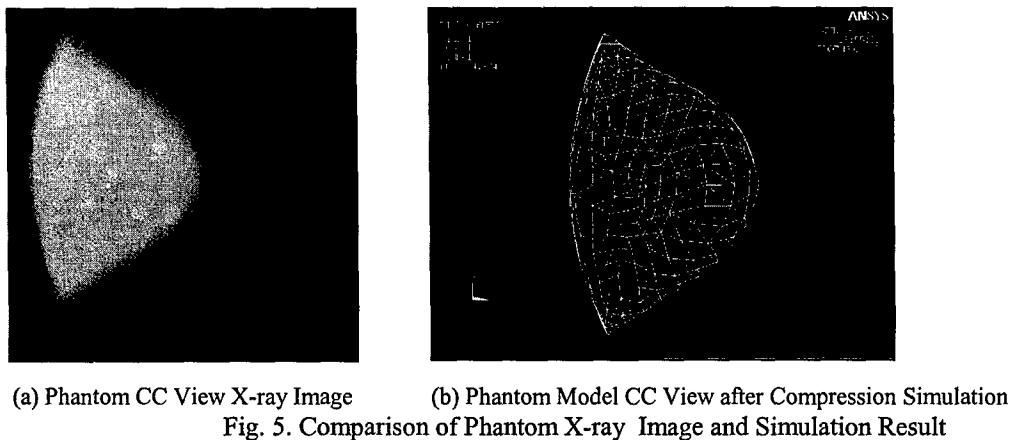


Fig. 5. Comparison of Phantom X-ray Image and Simulation Result

## 7. REFERENCES

- [1] R. G. Blanks, M. G. Wallis and R. M. Given-Wilson, "Observer variability in cancer detection during routine repeat (incident) mammographic screening in a study of two versus one view mammography," *J. Med. Screening*, 6, pp. 152-158, 1999.
- [2] R. M. Wilson and R. G. Blanks, "Incident Screening Cancers Detected with a second mammographic view: Pathological and radiological features," *Clinical Radiology*, vol. 54, pp. 724-735, 1999.
- [3] Paquerault, S., Petrick, N., Chan, H-P., Sahiner, B. and Helvie, M.A, "Improvement of computerized mass detection on mammograms: fusion of two-view information," *Med. Phys.* 29, pp. 238 – 247, 2002.
- [4] M. Yam, M. Brady, R. Highnam, C. Behrenbruch, R. English, Y. Kita, "3D reconstruction of microcalcification clusters from two mammographic views," *IEEE Trans. Medical Imaging*, 20, pp. 479-489, 2001
- [5] Bakic PR, Albert M, Brzakovic D, Maidment AD, "Mammogram synthesis using a 3D simulation. II. Evaluation of synthetic mammogram texture," *Med Phys.* 29(9), pp.2140-2551, 2002.
- [6] F. S. Azar, D. N. Metaxas, and M. D. Schnall, "A FEM of the breast for predicting mechanical deformation during biopsy procedures," *IEEE Workshop on Math. Methods in Biomedical Image Analysis*, pp. 38-45, 2000.

- [7] Schnabel, J.A.; Tanner, C.; Castellano-Smith, A.D.; Degenhard, A.; Leach, M.O.; Hose, D.R.; Hill, D.L.G.; Hawkes, D.J., "Validation of nonrigid image registration using FEM: application to breast MR images," *IEEE Trans. Medical Imaging*, 22(2), pp. 238-247, 2003.
- [8] Samani, A., J. Bishop, M.J. Yaffe, and D.B. Plewes, "Biomechanical 3-D finite element modeling of the human breast using MRI data," *IEEE Trans. Medical Imaging*, 20(4), pp. 271-279, 2001.
- [9] Duncan, J.S., "Geometrical and physical models for the recovery of quantitative information from medical image analysis," *Pattern Recognition*, 2002. Proceedings. 16th International Conference, 2, pp 277, 2002.
- [10] Y. Zhang, D. Goldgof and S. Sarkar, "Towards Physically-Sound Registration Using Object-Specific Properties for Regularization," *Second International Workshop on Biomedical Image Registration (WBIR '03)*, 2003.
- [11] L. Tsap, D. Goldgof, S. Sarkar, "Fusion of Physically-Based Registration and Deformation Modeling for Nonrigid Motion Analysis," *IEEE Trans. Image Processing*, 10(11), pp. 1659-1669, 2001.
- [12] S. Kumar, M. Sallam, D. B. Goldgof, "Matching point features under small nonrigid motion," *Pattern Recognition*, 34(12), pp. 2353-2365, 2001.
- [13] L. Tsap, D. Goldgof, S. Sarkar, "Nonrigid Motion Analysis Based on Dynamic Refinement of Finite Element Models," *IEEE Trans. Pattern Analysis and Machine Intelligence*, 22(5), pp. 526-543, 2000.
- [14] L. Tsap, D. Goldgof, S. Sarkar, P. Powers, "A Vision-Based Technique for Objective Assessment of Burn Scars," *IEEE Trans. Medical Imaging*, 17(4), pp. 620-633, 1998.
- [15] S. Anton, "A Finite Element Based Approach in Computer Vision and its Applications for Nonrigid Registration and Biometrics," Master Thesis, USF, 2002.
- [16] A. Singh, D. Goldgof, D. Terzopoulos, Editors, "Deformable Models in Medical Image Analysis," *IEEE Computer Society Press*, 1998.
- [17] Y. Qiu, D. Goldgof, L. Li, S. Sarkar, Yong Zhang, Sorin Anton. "Correspondence Recovery In 2-View Mammography," *IEEE ISBI*, 2004.
- [18] <http://www.ansys.com/>
- [19] I. Andersson, J. Hildell, A. Muhilow and H. Pettersson, "Number of projections in Mammography: Influence on Detection of Breast disease," *Am. J. Roentgenol.*, vol. 130, pp. 349-351, 1978.
- [20] R. Clark, R. Sutphen and C. Berman, "Breast cancer screening in high-risk women: Comparison of magnetic resonance imaging (MRI) with mammography," *H. Lee Moffitt Cancer Research Center*.
- [21] Y. Kita, R. Highnam and M. Brady, "Correspondence between different view breast X-rays using a simulation of breast deformation," *IEEE Proc. Computer Vision and Pattern Recognition*, pp. 700-707, 1998.
- [22] C. Kambhamettu, D. B. Goldgof, D. Terzopoulos, T. S. Huang, "Nonrigid Motion Analysis", in *Deformable Models in Medical Image Analysis*, Chapter 19, CS Press, 1998.
- [23] C. Kambhamettu, D. Goldgof, M. He, P. Laskov, "3D Nonrigid Motion Analysis under Small Deformations", *Image and Vision Computing*, 21(3), pp. 229-245, 2003.
- [24] R. M. Wilson and R. G. Blanks, "Incident Screening Cancers Detected with a second mammographic view: Pathological and radiological features," *Clinical Radiology*, vol. 54, pp. 724-735, 1999.
- [25] M. Yam, M. Brady, R. Highnam, C. Behrenbruch, R. English, and Y. Kita, "Three-dimensional reconstruction of microcalcification clusters from two mammographic views," *IEEE Trans. Medical Imaging*, vol. 20, pp. 479-489, 2001.
- [26] Y. Kita, R. Highnam and M. Brady, "Correspondence between different view breast x-rays using curved epipolar lines", *Computer Vision and Image Understanding*, vol. 83, pp. 38-56, 2001.